

gas. For example, by taking a leakage current density of  $1 \times 10^{-6} \text{ A cm}^{-2}$  as a reference of dielectric breakdown, the film deposited from the TEOS (15 sccm)/ $\text{C}_4\text{F}_8$  (16 sccm)/Ar mixture exhibits a breakdown strength of  $9.5 \text{ MV cm}^{-1}$  compared to  $5.1 \text{ MV cm}^{-1}$  for the film deposited from the TEOS (15 sccm)/Ar mixture. In addition, the  $\text{SiO}_2\text{:C:F}$  films have characteristics such as excellent thermal stability and water resistance.

## Experimental

$\text{SiO}_2\text{:C:F}$  films were deposited on clean Si substrates by using a conventional parallel plate electrode PE-CVD system. In the present study, the plasma was enhanced by a radio frequency (RF) of 13.56 MHz. The RF power was fixed at 160–200 W. The diameters of the top and bottom electrodes were 280 mm, the distance between them being adjustable in the range 13–27 mm. Water at about  $25^\circ\text{C}$  was circulated through the reaction chamber in order to maintain the reaction at room temperature. The Si wafers were placed on the bottom electrode plate, which rotated at about 10 rpm in order to improve the temperature distribution on the bottom electrode, and promote uniform thickness in the deposited film. All the films with a thickness of about 150 nm were deposited under a total pressure of 80 Pa, and the substrate was kept at room temperature.  $\text{C}_4\text{F}_8$  and TEOS were used as the reactant gases, and introduced into the reaction chamber through mass flow controllers. The  $\text{C}_4\text{F}_8$  flow rate was varied from 0 sccm to 27 sccm, TEOS vapor flow rate was kept at 15 sccm, and Ar was used as the balance gas. The TEOS liquid source was stored in a stainless steel container, and due to the relatively low process pressure, no carrier gas was used. In order to measure the capacitance–voltage ( $C$ – $V$ ) and current–voltage ( $I$ – $V$ ) characteristics, the films were deposited on the p-type Si(111) wafers with a resistivity of  $10^{-3} \Omega \text{ cm}$ , and aluminum electrodes with an area of  $1.5 \text{ mm}^2$  were evaporated on the deposited film to form a metal–insulator–semiconductor (MIS) structure. Another thin layer of aluminum was deposited on the back of the silicon substrate to assure ohmic contact between the back of the Si substrate and the stage of the prober.

Film thickness was measured using an ellipsometer with a He:Ne laser ( $\lambda = 632.8 \text{ nm}$ ). The FTIR spectra of the films were measured on an Avatar-360 IR spectrometer (Nicolet Co.). XPS measurements were made using a Perkin-Elmer PHI 5000c ESCA system with standard  $\text{Al K}\alpha$  radiation (1486.6 eV) at 93.90 eV of pass energy, and low magnification. The base pressure of the test chamber was  $10^{-9}$  torr. All the binding energies were calibrated by using  $\text{C}1s = 284.6 \text{ eV}$  as a reference point. Raman spectra were collected on an FT-Raman spectrometer (760 E.S.P.). The  $C$ – $V$  and  $I$ – $V$  characteristics of the films were measured with an LCR meter (Hewlett Packard Company, HP 4284A).

Received: October 20, 2000  
Final version: March 27, 2001

- [1] W. W. Lee, P. S. Ho, *MRS Bulletin* **1997**, 22, 19.
- [2] T. Homma, *Mater. Sci. Eng.* **1998**, R23, 243.
- [3] V. F. Dorfman, *Thin Solid Films* **1992**, 212, 267.
- [4] J. Z. Wan, F. H. Pollak, B. F. Dorfman, *J. Appl. Phys.* **1997**, 81, 6407.
- [5] P. Asokakumar, B. F. Dorfman, M. G. Abrazov, D. Yan, F. H. Pollak, *J. Vac. Sci. Technol. A* **1995**, 13, 1044.
- [6] Z. Y. Rong, M. Abrazov, B. Dorfman, M. Strongin, X.-Q. Yang, D. Yan, F. H. Pollak, *Appl. Phys. Lett.* **1994**, 65, 1379.
- [7] Y. Z. Zhou, S. Qin, C. Chan, P. K. Chu, *Mater. Res. Soc. Symp. Proc.* **1998**, 511, 63.
- [8] J. Lubguban Jr., A. Saitoh, Y. Kurata, T. Inokuma, S. Hasegawa, *Thin Solid Films* **1999**, 337, 67.
- [9] A. M. Wrobel, A. Walkiewicz-Pietrzykowska, S. Wickramanayaka, Y. Hatanaka, *J. Electrochem. Soc.* **1998**, 145, 2866.
- [10] S.-M. Yun, H.-Y. Chang, M.-S. Kang, C.-K. Choi, *Thin Solid Films* **1999**, 341, 109.
- [11] A. M. Wrobel, A. Walkiewicz-Pietrzykowska, M. Stasiak, J. Kulpinski, *Chem. Vap. Deposition* **1996**, 2, 285.
- [12] S.-J. Ding, P.-F. Wang, D. W. Zhang, J.-T. Wang, W. W. Lee, *J. Phys. D: Appl. Phys.* **2001**, 34, 155.
- [13] G. Lucovsky, J. Yang, S. S. Chao, J. E. Tyler, W. Czubytyj, *Phys. Rev. B: Condens. Matter* **1983**, 28, 3225.

- [14] L. He, T. Inokuma, Y. Kurata, S. Hasegawa, *J. Non-Cryst. Solids* **1995**, 185, 249.
- [15] G. Lucovsky, C. K. Wong, W. B. Pollard, *J. Non-Cryst. Solids* **1983**, 59–60, 839.
- [16] A. Vanhulsel, E. Dekempeneer, J. Smeets, J.-P. Celis, *J. Vac. Sci. Technol. A* **1999**, 17, 378.
- [17] J. Seth, S. V. Babu, *Thin Solid Films* **1993**, 230, 90.
- [18] H. Wieder, M. Cardona, C. R. Guarnieri, *Phys. Status Solidi B* **1979**, 92, 99.
- [19] M. Yoshimaru, S. Koizumi, K. Shimokawa, Y. Mori, H. Fukuda, N. Matsuki, *J. Vac. Sci. Technol. A* **1999**, 17, 425.
- [20] S. F. Durrant, S. G. C. Castro, L. E. Bolívar-Marinez, D. S. Galvão, M. A. B. Moraes, *Thin Solid Films* **1997**, 304, 149.
- [21] S. Agraharam, D. W. Hess, P. A. Kohl, S. A. B. Allen, *J. Vac. Sci. Technol. A* **1999**, 17, 3265.
- [22] J. Tanaka, C. F. Abrams, D. B. Graves, *J. Vac. Sci. Technol. A* **2000**, 18, 938.
- [23] W. S. Cho, Y. S. Oh, C. S. Kim, M. Osada, M. Kakihana, D. S. Lim, D. S. Cheong, *J. Alloys Compd.* **1999**, 285, 255.
- [24] A. Kakanakova-Georgieva, T. Marinova, O. Noblanc, C. Arnod, S. Cassette, C. Brylinski, *Thin Solid Films* **1999**, 337, 180.
- [25] G. Lucovsky, M. J. Manitini, J. K. Srivastava, J. P. Celis, *J. Vac. Sci. Technol. B* **1987**, 5, 530.
- [26] Y. Nakasaki, H. Miyajima, R. Katsumata, N. Hayasaka, *Jpn. J. Appl. Phys.* **1997**, 36, 2545.
- [27] K. Yamamoto, M. Tsuji, K. Washio, H. Kasahara, K. Abe, *J. Appl. Phys.* **1983**, 52, 925.
- [28] S. E. Alexandrov, M. L. Hitchman, *Chem. Vap. Deposition* **1997**, 3, 111.

## Liquid Source-MOCVD of $\text{Ba}_x\text{Sr}_{1-x}\text{TiO}_3$ (BST) Thin Films with a *N*-alkoxy- $\beta$ -ketoiminato Titanium Complex

By Yo-Sep Min,\* Young Jin Cho, Daesig Kim,  
Jung-Hyun Lee, Byong Man Kim, Sun Kwon Lim,  
Ik Mo Lee, and Wan In Lee

Owing to its high dielectric constant and low leakage current density,  $\text{Ba}_x\text{Sr}_{1-x}\text{TiO}_3$  (BST) is one of the promising dielectric materials for use in a capacitor in giga-bit dynamic random access memories (DRAMs).<sup>[1]</sup> For the successful fabrication of BST thin films by the liquid source metal–organic (LS-MO) CVD method, each precursor should have high volatility and an extended chemical or thermal stability at the vaporization temperature. In addition, precursors should decompose completely at the deposition temperature in order to avoid carbon contamination in the film.

Conventional Ti precursors for BST film deposition have been mainly alkoxides or  $\beta$ -diketonates, such as  $\text{Ti}(\text{O}^i\text{Pr})_4$ ,  $\text{Ti}(\text{thd})_2(\text{O}^i\text{Pr})_2$  (thd = 2,2,6,6-tetramethyl-3,5-heptanedione), and  $\text{Ti}(\text{mpd})(\text{thd})_2$  (mpd = 2-methyl-2,4-pentanedioxy). However, these precursors are not compatible with

[\*] Y.-S. Min, Y. J. Cho, Dr. D. Kim, Dr. J.-H. Lee, Dr. B. M. Kim  
Microelectronics Lab, Samsung Advanced Institute of Technology  
San #24, Nongseo-Ri, Kiheung-Eup,  
Yongin-City, Kyungki-Do, 449-900 (Korea)  
E-mail: ysmi@sait.samsung.co.kr  
S. K. Lim, Prof. I. M. Lee, Prof. W. I. Lee  
Department of Chemistry, Inha University  
#253, Yonghyun-Dong  
Nam-Gu, Incheon, 402-751 (Korea)

Ba or Sr precursors, such as Ba(thd)<sub>2</sub> and Sr(thd)<sub>2</sub>, in the preparation of BST films by LS-MOCVD. In a general semiconductor process, BST films are deposited at or below 430 °C to obtain good step coverage and surface uniformity for use in DRAM capacitors. At this low deposition temperature, however, Ti is poorly incorporated into BST films. It is possible that the  $\beta$ -diketonate ligands are not fully dissociated from the Ti metal ions, forming still-volatile varieties of partially decomposed Ti complexes, such as TiO(thd)<sub>2</sub>, due to the large charge-to-radius ratio of Ti (unlike the Ba or Sr precursors).<sup>[2]</sup> Thus, an excess amount of titanium precursor should be used to control the stoichiometry of BST thin films, however this often results in humps or a hazy appearance on the surface of BST films, (considered to be Ti-rich clusters).<sup>[3]</sup>

Recently,  $\beta$ -ketoimine compounds with aminoalkyl or polyether lariats have been utilized as a ligand of  $-1$  charge for group 2 or transition metals.<sup>[4-6]</sup> Even though the central metal ions of metal  $\beta$ -ketoiminate compounds,  $[M^{n+}(\beta\text{-ketoiminate})_n]$ , are coordinated with  $\beta$ -ketoiminates by chelation, such complexes are still sensitive to hydrolysis because the neutral amine or ether groups branched from  $\beta$ -ketoiminates are labile, due to rather weak bonds. For example, barium  $\beta$ -ketoiminate complexes with appended polyether lariats sublime with significant thermal decomposition.<sup>[7]</sup> In this study, *N*-alkoxy- $\beta$ -ketoiminates were used as terdentate ligands, of  $-2$  charge, for Ti metals in order to strengthen the metal-lariat bonds, and their application to the LS-MOCVD of BST thin films was investigated.

One *N*-alkoxy- $\beta$ -ketoiminato titanium complex, Ti(4-(2-methylethoxy)imino-2-pentanoate)<sub>2</sub>, [Ti(2meip)<sub>2</sub>], was synthesized by the route reported by Doherty et al.,<sup>[8]</sup> and successfully utilized as a metal-organic precursor of titanium for BST thin film deposition. As shown in Figure 1, since the vacant coordination sites of the central titanium

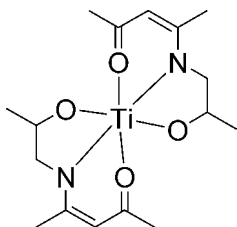


Fig. 1. Molecular structure of Ti(2meip)<sub>2</sub>.

ion of Ti(2meip)<sub>2</sub> are filled with terdentate ligands, showing enhanced chelate effect over bidentate ligands, this precursor has excellent chemical and thermal stability to such an extent that it remains structurally unchanged, even when left to stand in air for three months or more.

As demonstrated by thermogravimetric analysis (TGA) and differential scanning calorimetry (DSC), Ti(2meip)<sub>2</sub> melts at 199 °C and evaporates intact at around 290 °C in a one-step event under an N<sub>2</sub> atmosphere (Fig. 2a). The exothermic peak due to the decomposition of Ti(2meip)<sub>2</sub> in

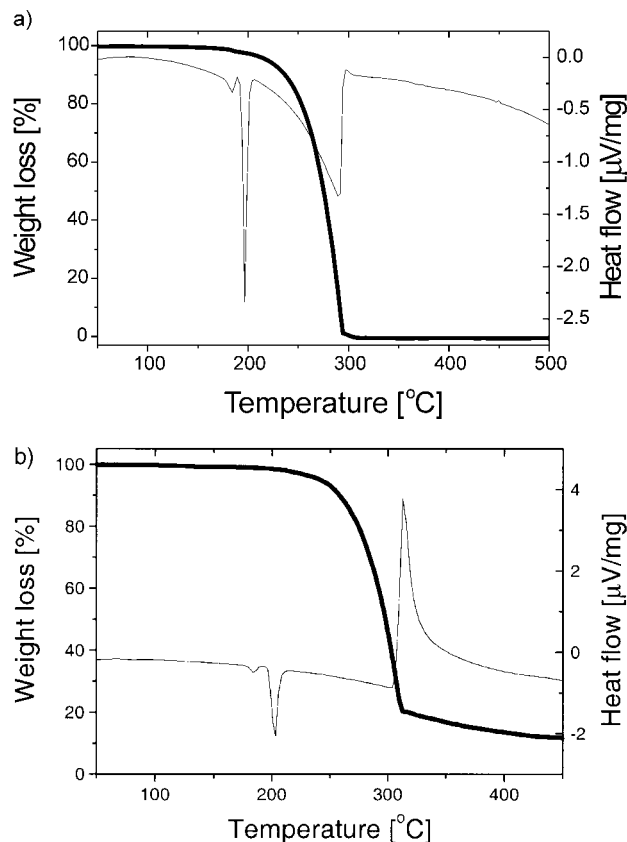


Fig. 2. Ambient pressure TGA (thick lines) and DSC (thin lines) of compound Ti(2meip)<sub>2</sub>, at a heating rate of 10 °Cmin<sup>-1</sup>: a) under a nitrogen atmosphere at a flow rate of 20 mL min<sup>-1</sup>, and b) under an air atmosphere at a flow rate of 30 mL min<sup>-1</sup>.

air appears to be sharp at 315 °C. This indicates that the decomposition mechanism of Ti(2meip)<sub>2</sub> is simple, and the complex easily decomposes, possibly due to the presence of a rather weak Ti–N bond and the homoleptic structure of the precursor (Fig. 2b). On the other hand, according to the TG-DSC thermogram (under an O<sub>2</sub> atmosphere) analyzed by Lee and Rhee, Ti(mpd)(thd)<sub>2</sub> shows a broad exothermic peak in the temperature range 300–380 °C, and Ti(thd)<sub>2</sub> (O'Pr)<sub>2</sub> decomposes in a two-step manner, showing exothermic peaks at around 275 °C and 356 °C.<sup>[9]</sup> In Figure 3, the sublimation rates of several Ti precursors are compared with Ba(methd)<sub>2</sub> [methd = 1-(2-methoxyethoxy)-2,2,6,6-tetramethyl-3,5-heptanedionate] and Sr(methd)<sub>2</sub>, employed in this work as the Ba and Sr precursors.<sup>[10]</sup> The sublimation rate of Ti(2meip)<sub>2</sub> is still higher than that of the Ba and Sr precursors, but appreciably lower than that of other conventional Ti precursors. Accordingly, the relatively low volatility of Ti(2meip)<sub>2</sub> may induce similar vaporization behavior in the Ba, Sr, and Ti precursors used in the deposition of a multi-component metal oxide such as BST thin film.

Figure 4 shows the morphology of the BST thin film deposited on Pt (1000 Å)/SiO<sub>2</sub> (1000 Å)/Si substrate with Ba(methd)<sub>2</sub>, Sr(methd)<sub>2</sub>, and Ti(2meip)<sub>2</sub> using LS-MOCVD. There are no humps and no hazy appearance on the surface

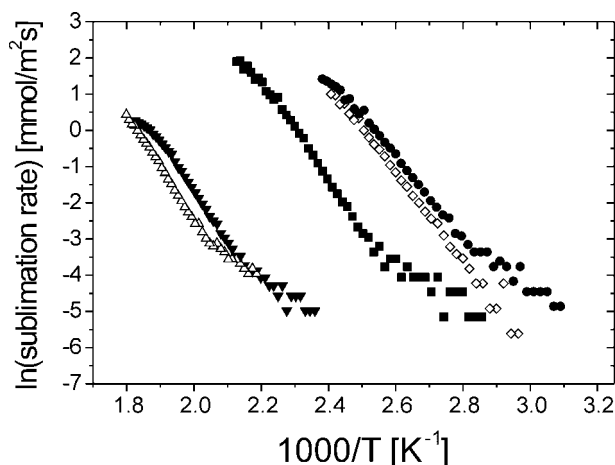


Fig. 3. TGA volatility comparison between  $\text{Ti}(\text{2meip})_2$ ,  $\text{Ti}(\text{thd})_2(\text{O'Pr})_2$ ,  $\text{Ti}(\text{mpd})(\text{thd})_2$ ,  $\text{Ba}(\text{methd})_2$ ,  $\text{Sr}(\text{methd})_2$ , and  $\text{Sr}(\text{methd})_2$ . Data were obtained under the following conditions: heating rate  $10^\circ\text{C min}^{-1}$  in vacuo ( $\sim 1$  torr).

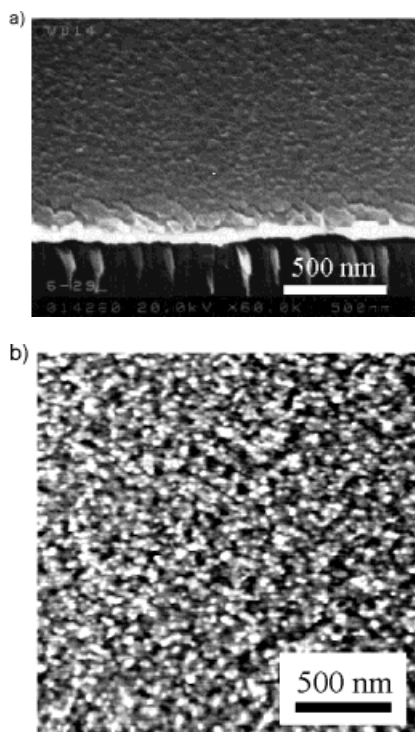


Fig. 4. a) Tilted SEM image and b)  $2 \times 2 \mu\text{m}^2$  AFM image, of the surface morphology of a 450 Å thick BST thin film grown on Pt (1000 Å)/ $\text{SiO}_2$  (1000 Å)/Si at  $430^\circ\text{C}$ . The rms roughness is 17 Å.

of the film grown at  $430^\circ\text{C}$ , and the root mean square (rms) roughness is only 17 Å. Moreover, the X-ray diffraction (XRD) patterns, denoted as (110) and (200) planes of the BST phase in Figure 5, indicate that the deposited films are beginning to crystallize at  $430^\circ\text{C}$ .

The temperature dependency of the titanium composition in the BST films is shown in Figure 6. When  $\text{Ti}(\text{2meip})_2$  was used as a Ti precursor, the composition of Ti in the BST film was not strongly dependent on the deposition

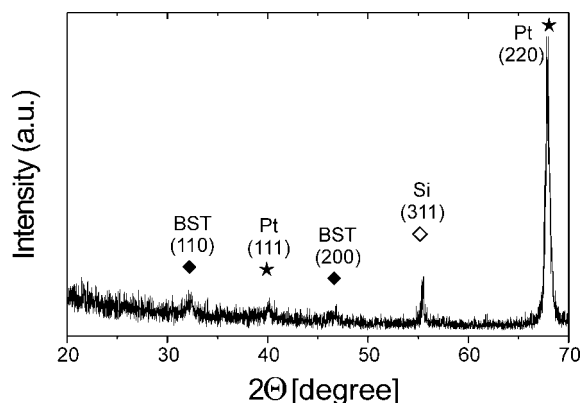


Fig. 5. XRD pattern of the as-deposited BST film grown on Pt (1000 Å)/ $\text{SiO}_2$  (1000 Å)/Si at  $430^\circ\text{C}$ .

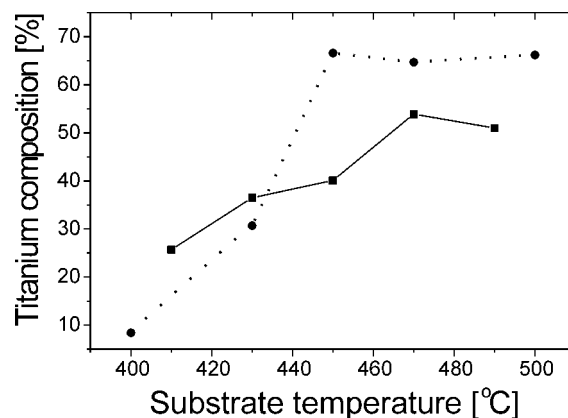


Fig. 6. Substrate temperature dependency of titanium composition defined as  $\text{Ti}/(\text{Ba} + \text{Sr} + \text{Ti})$ .  $\blacksquare$  and the solid line indicate the variation of titanium composition in BST films deposited with  $\text{Ti}(\text{2meip})_2$ , and  $\bullet$  and dotted line indicate that of  $\text{Ti}(\text{mpd})(\text{thd})_2$ .

temperature, unlike for  $\text{Ti}(\text{mpd})(\text{thd})_2$ . It is believed that the relatively easy and simple decomposition of  $\text{Ti}(\text{2meip})_2$  leads to an efficient incorporation of Ti into the BST film. This broadens the process window in terms of deposition temperature, and allows easy control of the titanium composition for the BST films, either over a large area, or in steps with a high aspect ratio.

In summary, an *N*-alkoxy- $\beta$ -ketoiminato titanium complex,  $\text{Ti}(\text{2meip})_2$ , shows excellent properties as a metal-organic precursor in terms of volatility, chemical and thermal stability, and decomposition behavior at around the deposition temperature. The BST films obtained from this precursor have an ultra-smooth surface without humps or hazy appearance, and relatively low dependency (compared with other titanium precursors) of the titanium composition on the deposition temperature.

## Experimental

$\text{Ba}_x\text{Sr}_{1-x}\text{TiO}_3$  thin films were deposited on Pt (1000 Å)/ $\text{SiO}_2$  (1000 Å)/Si substrate by LS-MOCVD, using  $\text{Ba}(\text{methd})_2$ ,  $\text{Sr}(\text{methd})_2$ , and  $\text{Ti}(\text{2meip})_2$ . Ba, Sr, and Ti precursors were dissolved in *n*-butyl acetate with the ratio

Ba/Sr/Ti = 1:1:8.6. The concentrations of Ba, Sr, and Ti precursors were 9.3 mM, 9.3 mM, and 80.0 mM, respectively. An input flow of the precursor solution was maintained at a rate of 0.05 mL min<sup>-1</sup> during the deposition. For the study of titanium incorporation as a function of substrate temperature, the depositions were carried out in a temperature range 400–500 °C, using the solution of Ba(methd)<sub>2</sub>, Sr(methd)<sub>2</sub>, and Ti(2meip)<sub>2</sub> (or Ti(thd)<sub>2</sub> (O<sup>i</sup>Pr)<sub>2</sub>) with the ratio Ba/Sr/Ti = 1:1:4.3. Deposition conditions for this study are summarized as follows; deposition pressure 1 torr, flow rate of carrier gas (N<sub>2</sub>) 100 sccm, flow rate of reaction gas (O<sub>2</sub>) 100 sccm and (N<sub>2</sub>) 100 sccm, vaporizer temperature 280 °C, deposition rate 30 Å min<sup>-1</sup> at 430 °C.

To analyze the atomic concentrations of barium, strontium, and titanium, the BST thin films were etched with hydrofluoric acid and then quantitatively analyzed by inductively coupled plasma-atomic emission spectroscopy (ICP-AES).

Received: December 18, 2000  
Final version: March 7, 2001

- [1] C. S. Hwang, S. O. Park, H.-J. Cho, C. S. Kang, H.-K. Kang, S. I. Lee, M. Y. Lee, *Appl. Phys. Lett.* **1995**, 67, 2819.
- [2] A. E. Turgambaeva, V. V. Krisyuk, I. K. Igumenov, S. V. Sysoev, *Chem. Vap. Deposition*, **2001**, 7, 121.
- [3] C. S. Kang, H.-J. Cho, C. S. Hwang, B. T. Lee, K.-H. Lee, H. Horii, W. D. Kim, S. I. Lee, M. Y. Lee, *Jpn. J. Appl. Phys.* **1997**, 36, 6946.
- [4] A. Bastianini, G. A. Battiston, F. Benetollo, R. Gerbasi, M. Porchia, *Polyhedron* **1997**, 16, 1105.
- [5] D. A. Neumayer, J. A. Belot, R. L. Feezel, C. Reedy, C. L. Stern, T. J. Marks, *Inorg. Chem.* **1998**, 37, 5625.
- [6] J. S. Matthews, O. Just. B. Obi-Johnson, W. S. Rees, Jr., *Chem. Vap. Deposition* **2000**, 6, 129.
- [7] D. B. Studebaker, D. A. Neumayer, B. J. Hinds, C. L. Stern, T. J. Marks, *Inorg. Chem.* **2000**, 39, 3148.
- [8] S. Doherty, R. J. Errington, N. Housley, J. Ridland, W. Clegg, M. R. J. Elsegood, *Organometallics* **1999**, 18, 1018.
- [9] J.-H. Lee, S.-W. Rhee, *J. Electrochem. Soc.* **2001**, 148, c409.
- [10] N. Kubota, A. Yoshinaka, A. Masuko, *Japanese Patent 9-136857*, **1997**.